J. Phys. B: At. Mol. Opt. Phys. 26 (1993) 2869–2878. Printed in the UK

Transition from quantum to quasi-classical behaviour of the binary encounter peak in collisions of 0.6 to 3.6 MeV amu^{-1} I^{23+} and Xe^{21+} with He and Ar

J L Shinpaugh†§, W Wolff†||, H E Wolf†||, U Ramm†, O Jagutzki†, H Schmidt-Böcking†, J Wang‡ and R E Olson‡

† Institut für Kernphysik, Universität Frankfurt, Frankfurt(M), Federal Republic of Germany
‡ Physics Department, University of Missouri-Rolla, Rolla, MO, USA

Received 23 October 1992, in final form 22 June 1993

Abstract. Double differential cross sections are reported for the production of binary encounter electrons in collisions of 0.6 MeV amu^{-1} I^{23+} and 1.4, 2.4, and 3.6 MeV amu^{-1} Xe^{21+} projectiles incident on He and Ar targets. Electron energy spectra were measured between 0° and 45° in the case of the two lower projectile energies, and between 17.5° and 60° for the two higher projectile energies. The data are compared with quantum mechanical impulse approximation and classical trajectory Monte Carlo calculations. While the quantum model calculation predicts a rapid disappearance of diffraction effects in the binary encounter peak with increasing projectile energy, these remain visible in the experimental results up to the highest energy measured. The necessity of including multiple target ionization involving inner shell electrons in the theoretical description of the collision process is demonstrated by the classical trajectory Monte Carlo calculation, which accounts well for the shape of the 2.4 and 3.6 MeV amu^{-1} cross sections, except at angles where diffraction effects are manifest. Systematic shifts of the binary encounter peak position towards lower energies with increasing emission angle were observed for all projectile energies.

1. Introduction

The production of binary encounter electrons in collisions involving partially stripped heavy ions has been the subject of a series of recent experimental and theoretical investigations. These studies were prompted by experimental evidence which suggested a behaviour of the binary encounter (BE) peak different from the expected classical behaviour described by two-body kinematics for the scattering of a free electron from a point projectile. The BE peak was studied by Richard *et al* (1990) at zero-degree observation angle for fluorine ions in several charge states colliding with H_2 and He at energies between 1 and 2 MeV amu^{-1}. Unexpectedly, a strong enhancement of the BE electron yield was observed for low charge states of the projectile as compared to the bare-ion Rutherford cross section. The angular dependence of the BE peak was studied for U^{33+} at 1.4 MeV amu^{-1} (Kelbch *et al* 1989), U^{21+} at 1.0 MeV amu^{-1} (Reinhold *et al* 1991), Au^{11+} at 0.6 MeV amu^{-1} (Hagmann *et al* 1992) and I^{7+}, I^{23+} and Au^{11+} at 0.6 MeV amu^{-1} (Wolff *et al* 1992). In all these cases, unexpected features of the electron emission spectra were encountered, either in the form of a sudden shift of the energy of the BE peak within a narrow angular interval, or in the

§ Present address: Oak Ridge National Laboratory, Oak Ridge, TN, USA.
|| Permanant address: Instituto de Fisica, Universidade Federal do Rio de Janeiro, Rio de Janeiro, Brazil.

0953-4075/93/172869+10$07.50

form of a splitting of that peak into two components. It was subsequently demonstrated that the origin of all these features lies in the non-Coulomb nature of the screened field of the projectile (Olson *et al* 1990, Shingal *et al* 1990, Reinhold *et al* 1990, 1991, Bhalla and Shingal 1991, Schultz and Olson 1991), which is responsible for both the zero-degree enhancement and the appearance of diffraction minima and maxima in the cross sections for elastic scattering of electrons in the projectile field. These diffraction effects, when incorporated into the impulse approximation, give rise to a non-classical angular behaviour of the BE peak which qualitatively reproduces the experimental results (Hagmann *et al* 1992, Wolff *et al* 1992).

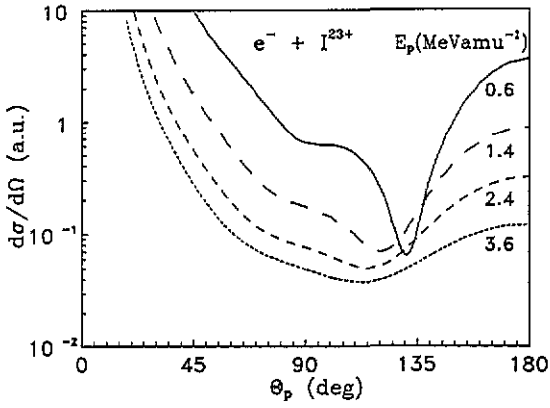

Figure 1. Calculated cross sections for the elastic scattering of electrons from I^{23+} for electron velocities corresponding to ion energies of 0.6, 1.4, 2.4 and 3.6 MeV amu^{-1}.

Systematic calculations of the cross sections for the elastic scattering of free electrons from partially stripped ions covering the mass range from carbon to uranium and an energy range from 0.1 to 5 MeV amu^{-1} have been published by Schultz and Olson (1991). The ionic potentials used in that work were based on the Hartree–Fock model potential of Garvey *et al* (1975). The cross sections show an enhancement over the bare-ion Rutherford value at 180° electron scattering angle (referring to the projectile frame of reference), which increases with decreasing ratio q/Z_p, where q and Z_p are the ionic and nuclear charge, respectively, of the projectile. At smaller scattering angles, there appears a succession of diffraction minima and maxima which become more numerous and more pronounced as the ion becomes heavier or more screened. As might be expected, the calculations also show, as a general tendency, that the interference effects become weaker with increasing electron energy. This tendency is demonstrated for the case of I^{23+} in figure 1, which shows the scattering cross sections for electrons with velocities equivalent to the projectile energies used in the present work of 0.6, 1.4, 2.4, and 3.6 MeV amu^{-1}. The cross sections were calculated using the method employed by Schultz and Olson (1991). The experimental basis with which to compare these extensive theoretical predictions, however, is still very limited.

The present work was undertaken in order to investigate in a more systematic way the energy dependence of these interference effects on the production of binary encounter electrons. The projectiles of I^{23+} and Xe^{21+} have been chosen, since the former had shown a strong interference effect in a previous investigation carried out at 0.6 MeV amu^{-1} (Wolff *et al* 1992).

2. Experimental arrangement

The 0.6 MeV amu^{-1} I^{23+} beam was obtained from the Emperor tandem Van de Graaff accelerator of the Max Planck Institut für Kernphysik, Heidelberg. Xe^{21+} beams with energies of 1.4, 2.4, and 3.6 MeV amu^{-1} were delivered by the UNILAC accelerator at GSI-Darmstadt. The experimental apparatus was essentially the same as that described by Kelbch *et al* (1992) and Wolff *et al* (1992). The ion beams traversed a differentially pumped gas cell, where the target gas pressure was kept within the 10^{-3} mbar range in order to assure single collision conditions, and were collected by a Faraday cup. The integrated beam charge was used to advance the voltage applied to the electrostatic electron spectrometer. Energy spectra of secondary electrons were measured with a 127° cylindrical spectrometer in the case of the 0.6 and 1.4 MeV amu^{-1} beams, and with a double-focusing hemispherical sector analyser for the two higher-energy beams. While the cylindrical spectrometer covered the entire angular range down to 0°, the lowest possible angle of the hemispherical sector analyser was mechanically limited to 17.5°. Angular and energy resolution of both spectrometers were set to ±1° and 5%, respectively.

3. Results and discussion

The double differential cross sections (DDCS) for secondary electron emission from 0.6 MeV amu^{-1} I^{23+} and 1.4 MeV amu^{-1} Xe^{21+} incident on Ar are shown in figures 2(*a*) and 2(*b*) for emission angles from 0° to 40° with respect to the beam. The cross sections for 2.4 and 3.6 MeV amu^{-1} Xe^{21+} incident on He are shown in figures 2(*c*) and 2(*d*) for the angular range from 17.5° to 50°. It was found that different noble gases give rise to cross sections differing essentially by overall scaling factors, a fact which has been noted previously for the case of Au^{11+} projectiles (Hagmann *et al* 1992).

At the two lower projectile energies of 0.6 and 1.4 MeV amu^{-1}, the non-classical behaviour of the binary encounter peak is strongly evident in the experimental results. For 0.6 MeV amu^{-1}, the peak is located at approximately 1000 eV at very forward angles from 0° to 17.5°, and at 700 eV at larger angles from 27.5° to 35°. There is no smooth angular dependence of the energy of the peak, such as would be expected from purely kinematical considerations for two-body scattering of a free electron, which would have an energy $E = 4(m_e/M_P)E_P\cos^2\theta_L$, where m_e and M_P are respectively the electron and projectile masses, E_P is the projectile energy, and θ_L is the electron emission angle in the laboratory frame. Instead, the position of the peak shows little variation with θ_L except in the narrow angular region of 20° to 25° where the energy shift of the BE peak takes place. In this range, there is so little BE peak intensity that only featureless exponentially decreasing cross sections can be observed. This same behaviour is also found at 1.4 MeV amu^{-1}, except that a slight continuous displacement of the BE peak, apart from the sudden shift at 27.5°, can be observed over the entire angular range studied.

This same sudden shift in the position of the binary peak, now occurring at about 30°, is still well discernible at the next higher projectile energy of 2.4 MeV amu^{-1}, although the binary peak no longer disappears at the angle where the shift takes place. In addition, the continuous displacement, already noted at 1.4 MeV amu^{-1}, is now more pronounced. At the highest measured energy of 3.6 MeV amu^{-1}, a close inspection of the shape of the binary peak still reveals a slight broadening at 30° and 35°. Otherwise a smooth displacement resembling (but not matching) that given by the formula for free-electron scattering completely dominates the angular dependence of the BEP.

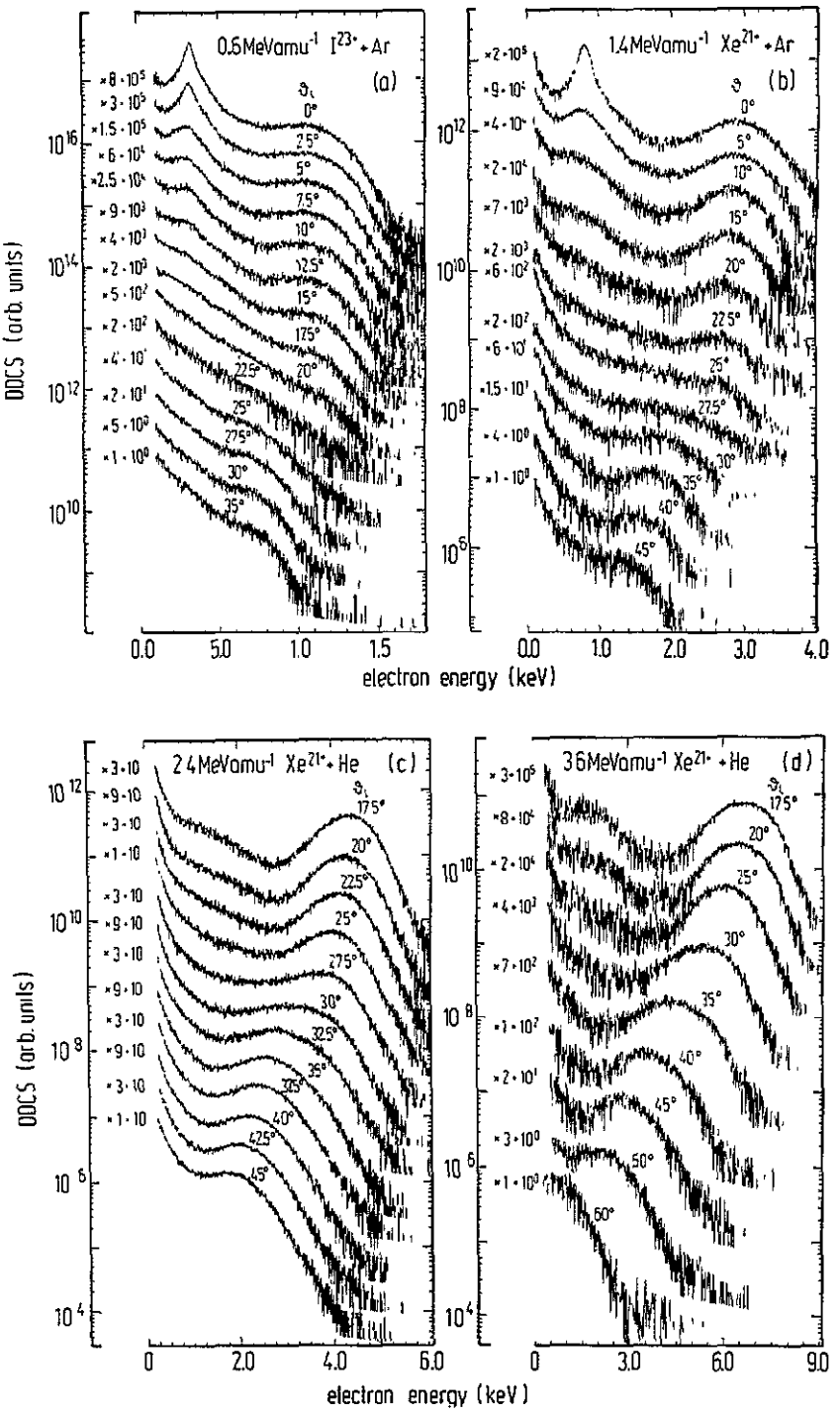

Figure 2. Measured double differential cross sections (DDCS) for secondary electron emission for the collision systems of (*a*) 0.6 MeV amu^{-1} I^{23+} incident on Ar, (*b*) 1.4 MeV amu^{-1} Xe^{21+} incident on Ar, (*c*) 2.4 MeV amu^{-1} Xe^{21+} incident on He and (*d*) 3.6 MeV amu^{-1} Xe^{21+} incident on He.

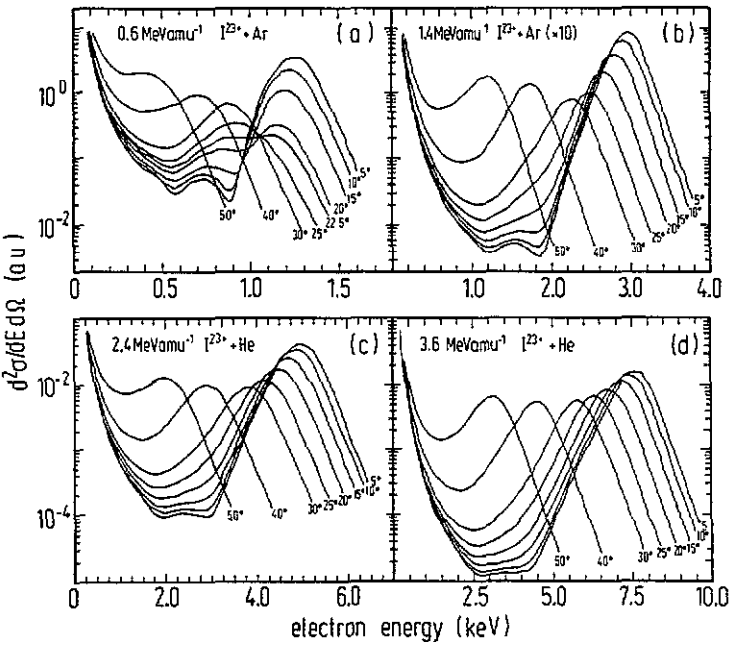

Figure 3. Double differential cross sections for binary encounter electron production calculated within the impulse approximation for I^{23+} incident on Ar for projectile velocities of (*a*) 0.6 and (*b*) 1.4 MeV amu^{-1} and incident on He for projectile velocities of (*c*) 2.4 and (*d*) 3.6 MeV amu^{-1}.

Model calculations for binary encounter electron production were performed within the framework of the impulse approximation (IA) using a method adapted from the one previously employed by Wang *et al* (1991) for treating electron loss. In the projectile reference frame, the binary encounter cross section is calculated by convoluting the cross section for elastic scattering of the target electrons in the projectile field with the initial momentum distribution (Compton profile) of the target electron. Momentum and energy conservation allow only a restricted subset of momenta to contribute to a given final electron momentum. The elastic scattering cross section is calculated by partial wave expansion in the field of the projectile. The resulting cross section is then transformed into the laboratory frame of reference. In the case of Ar, only the 3p target electrons are included in the calculation. The results are shown in figures 3(*a*)–(*d*) in the form of double differential cross sections for the four projectile energies.

As can be seen from the calculated BE peak shapes, a much swifter disappearance of diffraction effects, with increasing projectile energy, is predicted by the impulse approximation than is observed in the experimental results. At the lowest projectile energy (figure 3(*a*)), diffraction effects strongly mark their presence in the form of pronounced minima and maxima which compose the BE peak. These do not appreciably change their position with θ_L. Rather, the BE intensity shifts gradually from one maximum to the next with changing angle. The BE peak intensity passes through a minimum at an angle of 22.5°, accompanied by a shift of intensity from the higher-energy peak to the lower-energy peak. The minimum in the binary encounter intensity is a consequence of the deep diffraction minimum present at 132° in the 0.6 MeV amu^{-1} electron scattering cross section of figure 1. This predicted behaviour agrees well with the 0.6 MeV amu^{-1} data.

At the next higher energy of 1.4 MeV amu^{-1} (figure 3(*b*)), the calculated binary peak

intensity still passes through a minimum, now located at an angle of about 30°, although the peak shape no longer exhibits the signs of interference structure observed at the lower projectile energy of 0.6 MeV amu^{-1}. As in the previous case, this minimum in the intensity is caused by a diffraction minimum in the 1.4 MeV amu^{-1} electron scattering cross section (figure 1), now located at a projectile frame angle of 120°. A discontinuous shift in position of the BE peak, however, is no longer to be expected from the calculation. The data, on the other hand, show about the same degree of 'quantal' behaviour as do the 0.6 MeV amu^{-1} results. At the projectile energy of 2.4 MeV amu^{-1}, the calculated cross sections decrease between 30° and 40°, i.e., the BE peak intensity exhibits a shallow minimum in this region, but otherwise the peak position follows a $\cos^2\theta_L$ dependence. The minimum in BE peak intensity at intermediate angles has practically disappeared at the highest energy of 3.6 MeV amu^{-1}.

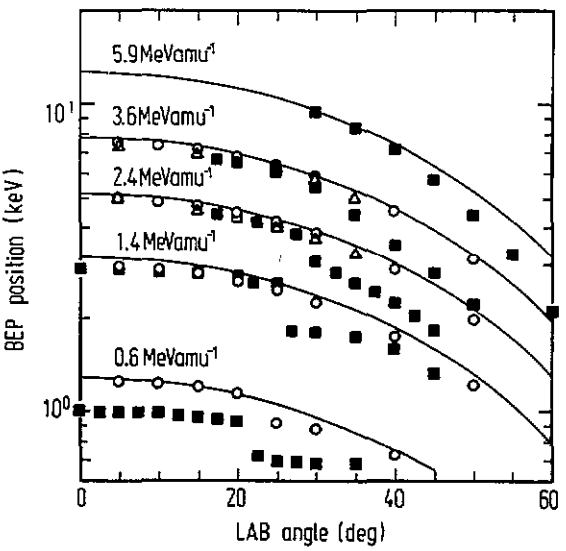

Figure 4. Binary encounter peak (BEP) energy as a function of the angle of observation, θ_L, for projectile energies of 0.6, 1.4, 2.4, 3.6 and 5.9 MeV amu^{-1}. Full curve, free-electron scattering; ○, impulse approximation; △, *n*CTMC; ■, experimental results.

For closer examination of the angular dependence of the energy of the binary encounter peak, figure 4 shows the experimentally observed position of the BE peak as a function of θ_L for the four projectile energies. Results for the higher projectile energy of 5.9 MeV amu^{-1} from Ramm (1992) have been included. The figure also contains the BE peak energy for scattering of a free electron, as well as the energy from the impulse approximation and from an *n*-body classical trajectory Monte Carlo (*n*CTMC) calculation performed for the 2.4 and 3.6 MeV amu^{-1} collision systems. The transition from quantal behaviour at low projectile energies, characterized by the combination of near constancy of the BE peak energy over large angular ranges and sudden shifts within a small angular interval, to almost classical behaviour at higher energies, characterized by a smooth angular dependence of this energy, is well borne out in the curves of figure 4; however, the IA calculation predicts a swifter disappearance of quantum diffraction effects with increasing projectile energy than shown by experiment.

The impulse approximation gives a BE peak energy which is very close to the free-electron value at all angles and all projectile energies except the lowest one. This is also

the case for the energies calculated with the *n*CTMC method for 2.4 and 3.6 MeV amu^{-1}. At 0.6 MeV amu^{-1} projectile energy, the BE peak was experimentally observed to be located considerably below the predicted values. At the higher projectile energies, experimental and calculated energies of the BE peak agree at small angles, but the experimental peak energy always decreases with increasing angle faster than expected from the calculations. Recent studies of the BE peak at 0° have shown shifts in the energy of the BE peak for highly charged bare projectiles due to binding energy or two-centre effects (Lee *et al* 1990, Miraglia and Macek 1991, Schultz and Olson 1991, Pedersen *et al* 1991, Fainstein *et al* 1992), but no model at present predicts shifts which are angular dependent.

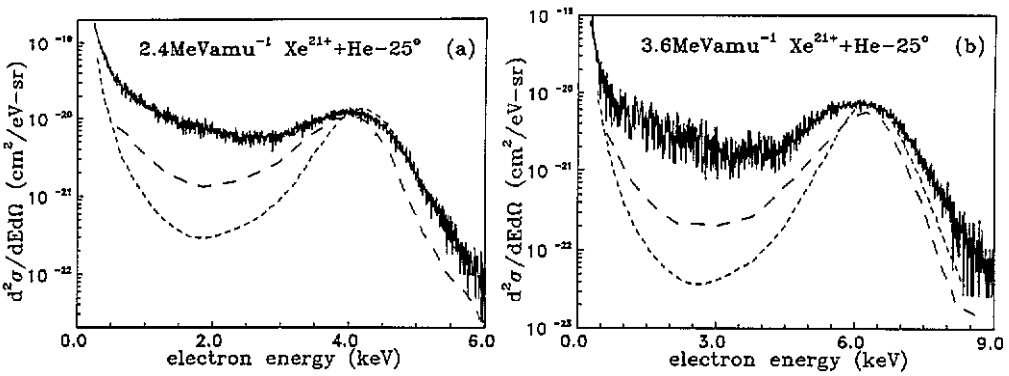

Figure 5. Double differential cross sections for secondary electron emission in collisions of (*a*) 2.4 MeV amu^{-1} and (*b*) 3.6 MeV amu^{-1} Xe^{21+} incident on He at an observation angle θ_L=25°. Full curve, experiment; long-broken curve, *n*CTMC; short-broken curve, impulse approximation.

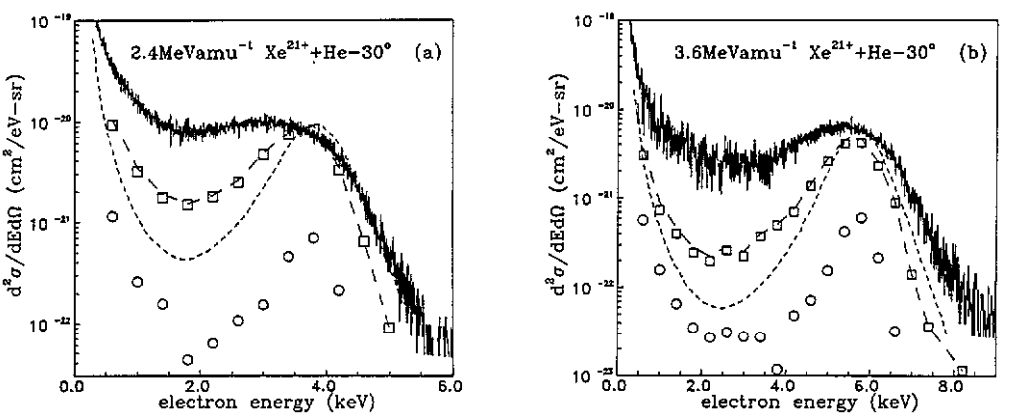

Figure 6. The same as figure 5, but for θ_L=30°. In addition, the single and double ionization cross sections from the *n*CTMC calculation are given separately. □, double-ionization cross section; ○, single-ionization cross section.

For a more direct comparison between theoretical and experimental double differential cross sections, the experimental results were normalized to the impulse approximation at the BE peak maximum, and are presented in figures 5 and 6 for the observation angles of

25° and 30°, respectively, for the two higher projectile energies. The *n*CTMC results have also been included. At 25° (figure 5), the *n*CTMC cross sections account reasonably well for the width of the BE peak and for the continuum of intermediate-energy (between the cusp and the BE peak) and low-energy electrons, while the impulse approximation underestimates the width of the peak by failing to reproduce its low-energy tail. These intermediate-energy electrons originate from non-binary processes where two-centre potential scattering must be taken into account, as done in the *n*CTMC calculation.

At 30° for the projectile energy of 2.4 MeV amu^{-1} (figure 6(*a*)), the shape of the BE peak is not well reproduced by the impulse approximation or the *n*CTMC calculation. The reason for this failure of the classical *n*CTMC calculation is, of course, that at 30° the experimental BE peak is broadened by diffraction effects. However, this feature also is not reproduced by the quantum mechanical impulse approximation calculation.

For the projectile energy of 3.6 MeV amu^{-1} (figure 6(*b*)), the *n*CTMC calculation still gives a reasonable account of the width of the BE peak, although it is somewhat underestimated. Also shown in figure 6 is the contribution to the *n*CTMC cross sections from each target recoil ion charge state. A comparison between the *n*CTMC single and total ionization cross sections reveals that the low-energy asymmetry of the BE peak is only reproduced when double-ionization processes are taken into account. In fact, the cross section leading to double ionization of He is an order of magnitude larger than the single ionization cross section, i.e., most probably the target is left fully ionized in collisions producing binary encounter electrons. These multiple-ionization processes are not incorporated into the impulse approximation. That these processes are important becomes clear when a heavy target is considered.

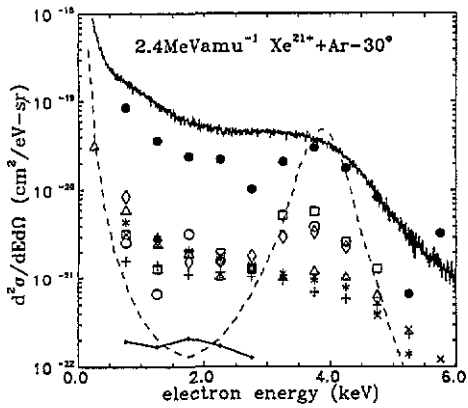

Figure 7. Double differential cross sections for secondary electron production in collisions of 2.4 MeV amu^{-1} Xe^{21+} incident on the Ar system for θ_L=30°. Full curve, experiment; broken curve, impulse approximation. The following symbols give the contribution from each target final charge state Ar^{q+} to the secondary electron cross section as calculated by the *n*CTMC method: ○, $q = 2+$; □, $q = 4+$; ◇, $q = 6+$; △, $q = 8+$; ∗, $q = 10+$; ×, $q = 12+$; +, $q = 14+$; ○, $q = 16+$; ●, total ionization.

The results of an *n*CTMC calculation for electron emission at 30° for 2.4 MeV amu^{-1} Xe^{21+} incident on Ar are compared with the impulse approximation and the experimental results in figure 7. The *n*CTMC cross sections for different final charge states of the residual target Ar^{q+} ($q = 2$–16) are shown. The calculated total cross sections (contributions from all charge states) show good agreement with the experimental results. The charge states which contribute to the BE peak are observed to be the 2+, 4+, and 6+ states (i.e., ionization events involving only the 3p shell electrons). Charge states from 4+ up to 14+ all give similar contributions to the yield of intermediate-energy electrons between the binary encounter peak and the cusp. The broad electron energy distributions in coincidence with these highly charged recoils are to be expected, since tightly bound inner shell electrons possessing a broad initial momentum distribution are removed. In addition, if initial ionization occurs at

large distances before the ejection of a fast electron, the electrons in the outer shells may have time to relax, becoming more tightly bound, thus leading to a broader BE peak.

It is therefore important to include the electrons from inner shells into the description of the double differential cross sections. For highly charged projectiles, multiple ionization events leading to high recoil charges contribute significantly to the double differential cross sections in the intermediate electron energy range, while contributions to the BE peak come predominantly from lower charge states. The resulting effect, then, is a broader BE peak than would be expected from the ionization of a single electron from an outer shell, as seen in the impulse approximation.

4. Concluding remarks

A systematic experimental and theoretical investigation of the energy dependence of diffraction effects in the binary encounter peak has been presented for collisions of I^{23+} and Xe^{21+} projectiles with He and Ar targets in the energy range from 0.6 to 3.6 MeV amu^{-1}. The experimental results were compared to quantum mechanical impulse approximation and classical *n*CTMC calculations. While the impulse approximation gives a satisfactory description of the observed diffraction effects at low projectile energies, it fails to do so at higher energies by predicting too swift a disappearance of these effects and the onset of a behaviour of the binary encounter peak typical for unscreened projectiles. An angular-dependent energy shift of the position of the binary encounter peak not accounted for by the impulse approximation and the *n*CTMC calculations was observed. The width of the binary encounter peak at angles where diffraction effects are not present, as well as the intermediate-energy electrons, are reasonably well described by the *n*CTMC calculation. It was demonstrated in this calculation that multiple target ionization plays an important role in secondary electron emission in these highly charged collision systems.

Acknowledgments

We would like to acknowledge stimulating conversations with Professors C L Cocke and S Hagmann. Two of the authors gratefully acknowledge financial support received during the course of the present investigation: JLS to the Alexander von Humboldt Foundation and the Fulbright Commission and HEW to the Conselho Nacional de Desenvolvimento Cientifico e Tecnologico (Brazil). Support by BMFT and DFG is also acknowledged.

References

Bhalla C P and Shingal R 1991 *J. Phys. B: At. Mol. Opt. Phys.* **24** 3187

Fainstein P D, Ponce V H and Rivarola R D 1992 *Phys. Rev.* A **45** 6417

Garvey R H, Jackmann C H and Green A E S 1975 *Phys. Rev.* A **12** 1144

Hagmann S, Wolff W, Shinpaugh J L, Wolf H E, Olson R E, Bhalla C P, Shingal R, Kelbch C, Herrmann R, Jagutzki O, Dörner R, Koch R, Euler J, Ramm U, Lencinas S, Dangendorf V, Unverzagt M, Mann R, Mokler P, Ullrich J, Schmidt-Böcking H and Cocke C L 1992 *J. Phys. B: At. Mol. Opt. Phys.* **25** L287

Kelbch C, Hagmann S, Kelbch S, Mann R, Olson R E, Schmidt S and Schmidt-Böcking H 1989 *Phys. Lett.* **139A** 304

Kelbch C, Koch R, Hagmann S, Ullmann K, Schmidt-Böcking H, Reinhold C O, Schultz D R, Olson R E and Kraft G 1992 *Z. Phys.* D **22** 713

Lee D H, Richard P, Zouros T J M, Sanders J M, Shinpaugh J L and Hidmi H 1990 *Phys. Rev.* A **41** 4816

Miraglia J E and Macek J 1991 *Phys. Rev.* A **43** 5919
Olson R E, Reinhold C O and Schultz D R 1990 *J. Phys. B: At. Mol. Opt. Phys.* **23** L455
Pedersen J O, Hvelplund P, Petersen A G and Fainstein P D 1991 *J. Phys. B: At. Mol. Opt. Phys.* **24** 4001
Ramm U 1992 Private communications
Reinhold C O, Schultz D R and Olson R E 1990 *J. Phys. B: At. Mol. Opt. Phys.* **23** L591
Reinhold C O, Schultz D R, Olson R E, Kelbch C, Koch R and Schmidt-Böcking H 1991 *Phys. Rev. Lett.* **66** 1842
Richard P, Lee D H, Zouros T J M, Sanders J M and Shinpaugh J L 1990 *J. Phys. B: At. Mol. Opt. Phys.* **23** L213
Schultz D R and Olson R E 1991 *J. Phys. B: At. Mol. Opt. Phys.* **24** 3409
Shingal R, Chen Z, Karim K R, Lin C D and Bhalla C P 1990 *J. Phys. B: At. Mol. Opt. Phys.* **23** L637
Wang J, Reinhold C O and Burgdörfer J 1991 *Phys. Rev.* A **44** 7243
Wolff W, Shinpaugh J L, Wolf H E, Olson R E, Wang J, Lencinas S, Piscevic D, Herrmann R and Schmidt-Böcking H 1992 *J. Phys. B: At. Mol. Opt. Phys.* **25** 3683